Supporting Information

Flexible Self-Powered Real-Time Ultraviolet Photodetector by Coupling Triboelectric and Photoelectric Effects

Yi Zhang[1,δ], Mingfa Peng[2,δ], Yina Liu[3,], Tingting Zhang[1], Qianqian Zhu[1], Hao Lei[1], Sainan Liu[1], Yi Tao[1], Long Li[4], Zhen Wen[1,*] and Xuhui Sun[1,*]*

[1] Institute of Functional Nano and Soft Materials (FUNSOM), Jiangsu Key Laboratory for Carbon-Based Functional Materials and Devices, Soochow University, Suzhou 215123, China.

[2] College of Electronic and Information Engineering, Changshu Institute of technology, Changshu 215500, China

[3] Department of Mathematical Sciences, Xi'an Jiaotong-Liverpool University, Suzhou 215123 China.

[4] Suzhou Institute of Metrology, Suzhou, China.

[δ] Y.Z. and M.P. contributed equally to this work.

* Corresponding Authors: yina.liu@xjtlu.edu.cn (Y. Liu); wenzhen2011@suda.edu.cn (Z. Wen); xhsun@suda.edu.cn (X. Sun)

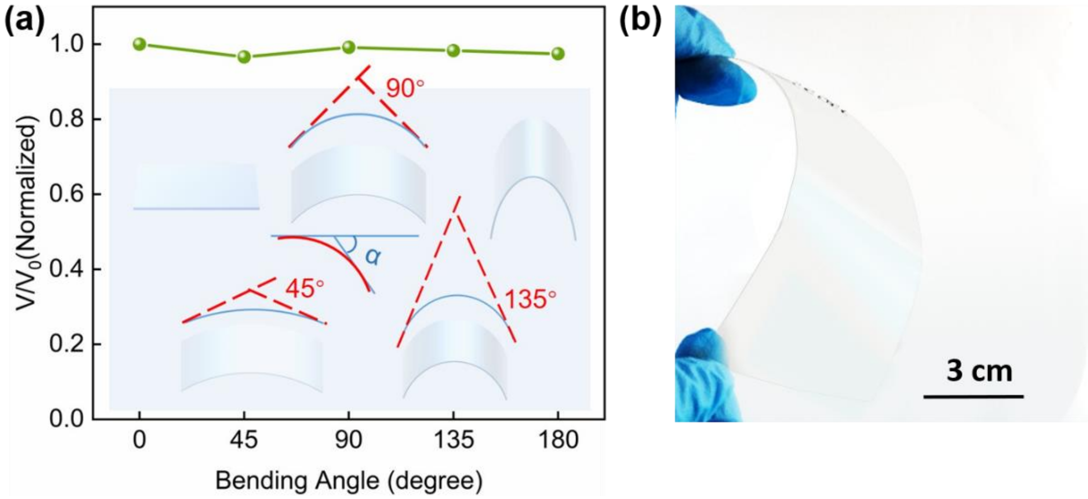

Figure S1. (a) Stability of the TFF-TENG after bengding for 50,000 cycles. (b) Photograph of the self-powered UV photodetector.

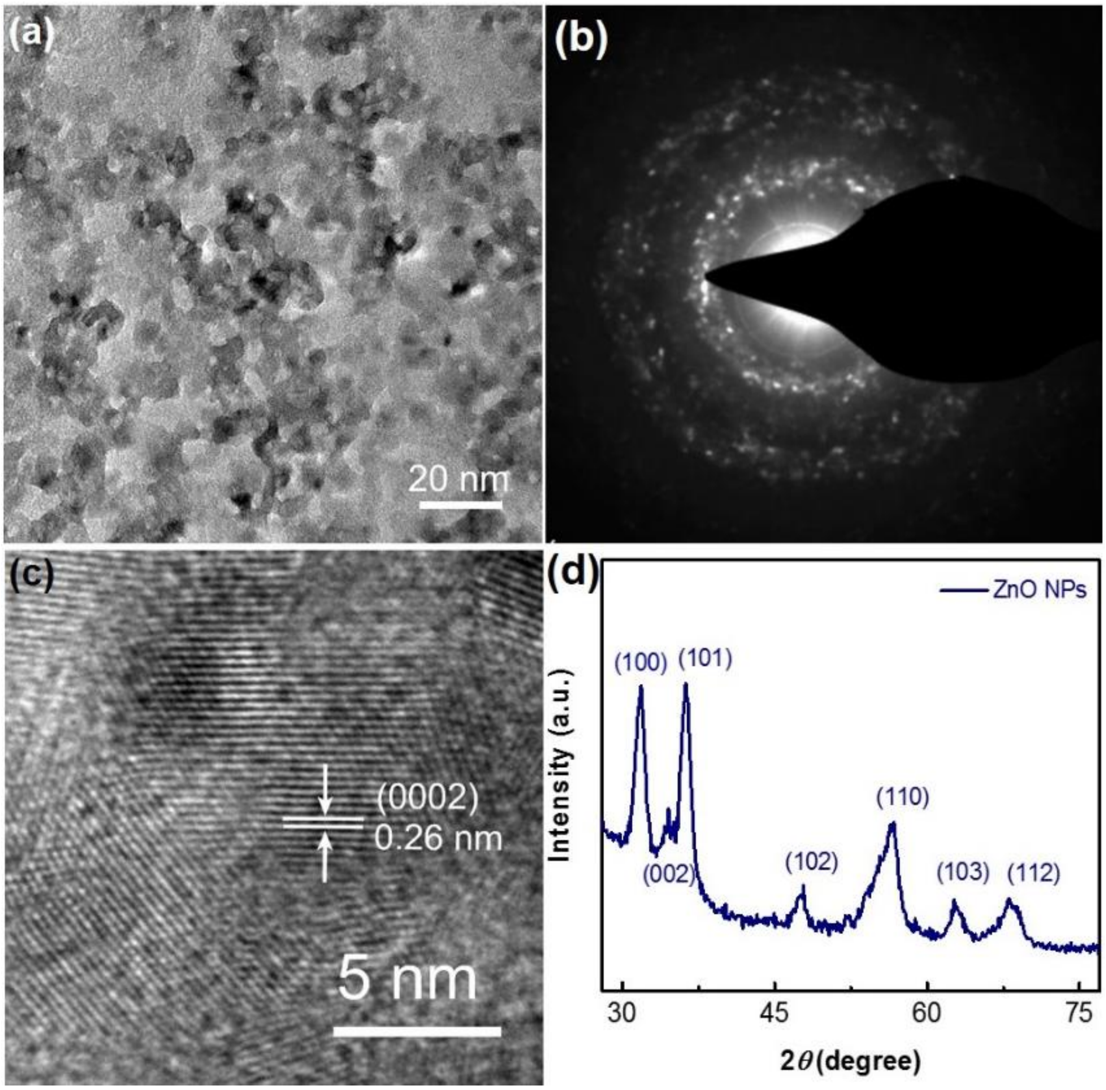

Figure S2. Characterization of the as-synthesized ZnO nanoparticles (NPs). (a) TEM image, (b) selected area electron diffraction (SAED) image, (c) HRTEM image and (d) XRD pattern of the ZnO NPs.

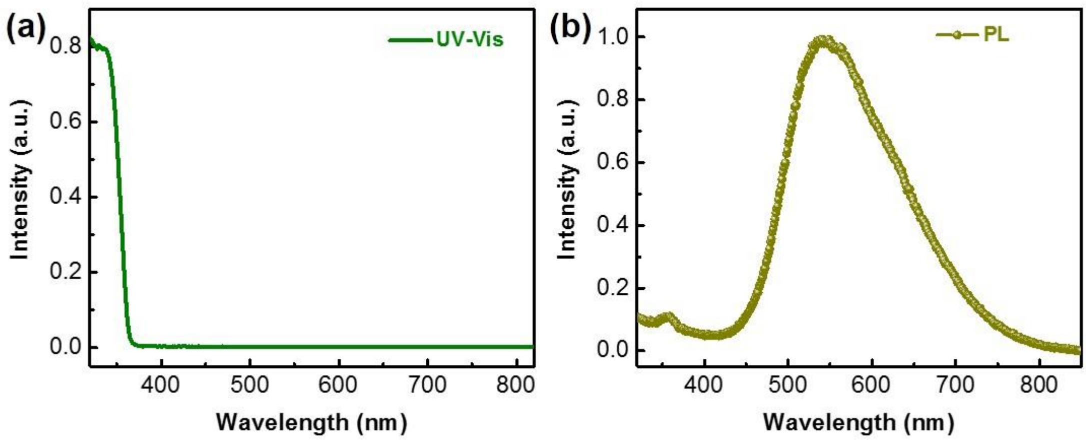

Figure S3. (a) UV-Vis spectra of the ZnO NPs. (b) PL spectra of the ZnO NPs.

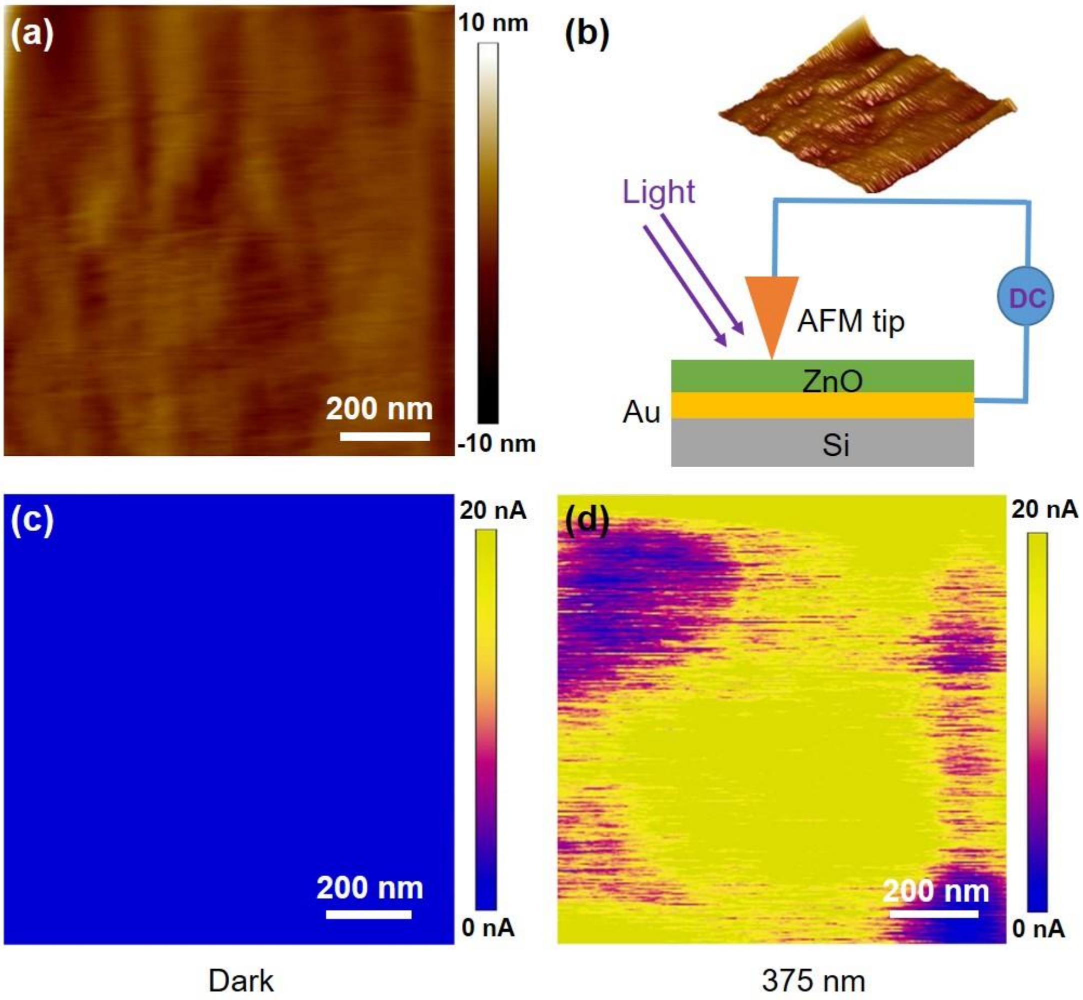

Figure S4. (a) Surface morphology of ZnO NPs films characterized by AFM. (b) The schematic diagram of photoelectric properties of ZnO NPs tested by C-AFM mode; the upper corner illustration is the corresponding three-dimensional morphology image. Current map of ZnO NPs (c) under dark condition and (d) UV light at 375 nm with the current resolution of nA.

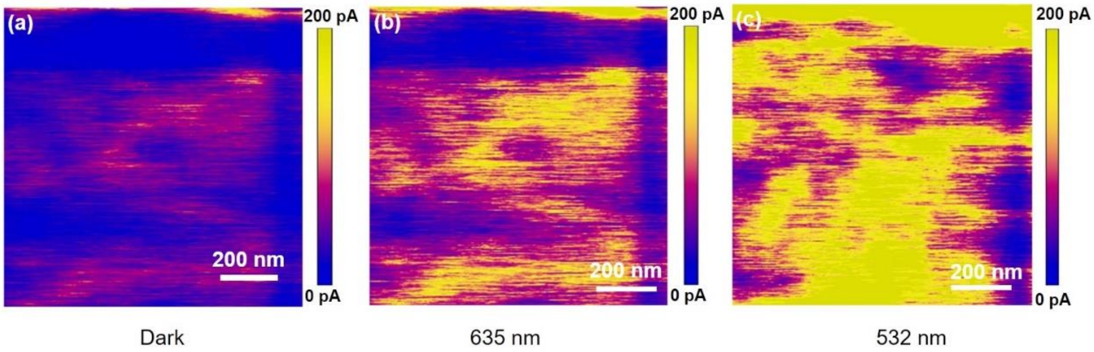

Figure S5. Current map of ZnO NPs under (a) dark , (b) 635nm, and (c) 532 nm visible light illumination with the current resolution of pA.

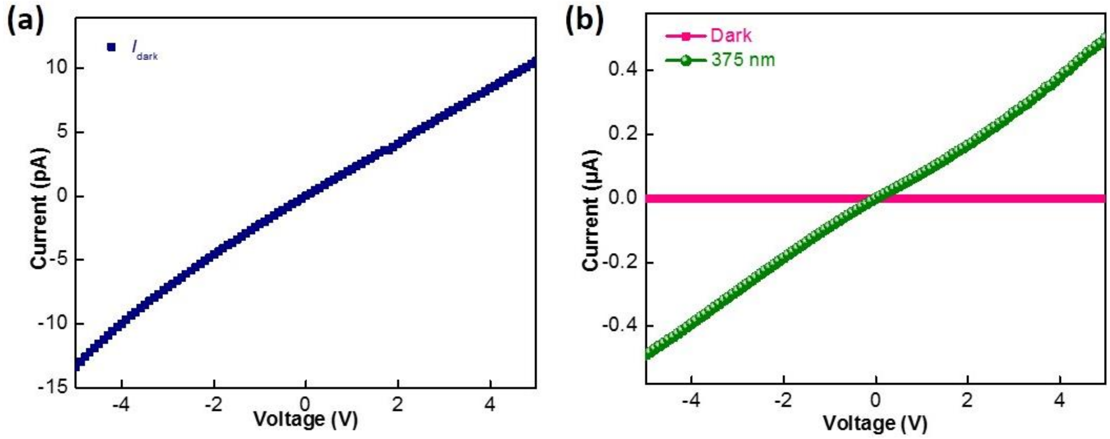

Figure S6. *I-V* curves of the ZnO UV photodetector (a) under dark and (b) 375 nm UV light with power intensities irradiance of 31.92 mW/cm^2.

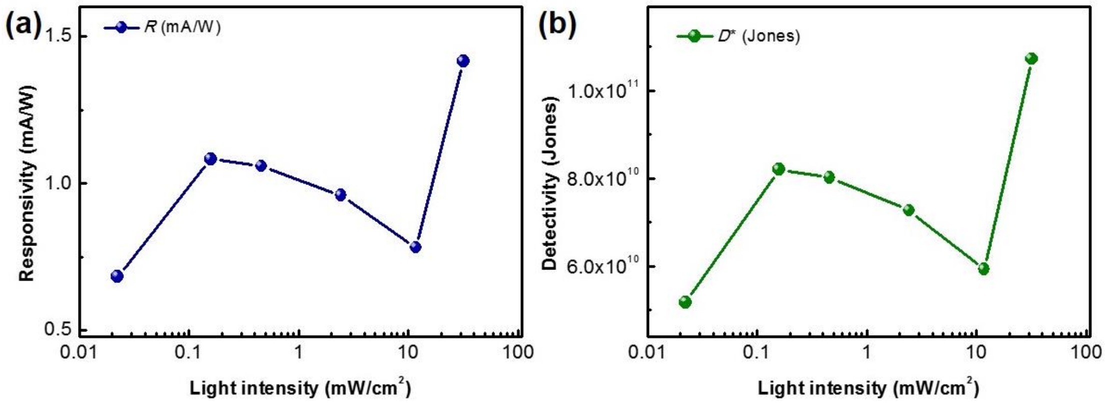

Figure S7. (a) Responsivity and (b) specific detectivity of the photodetector under 375 nm light illumination at the bias of 5 V.

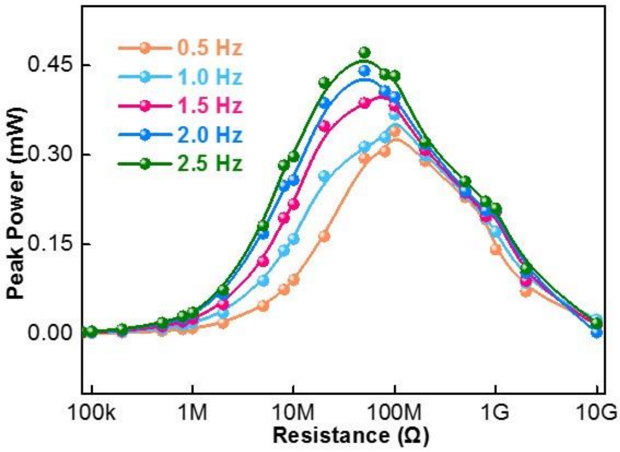

Figure S8. Peak power density under varies frequencies in taping mode.

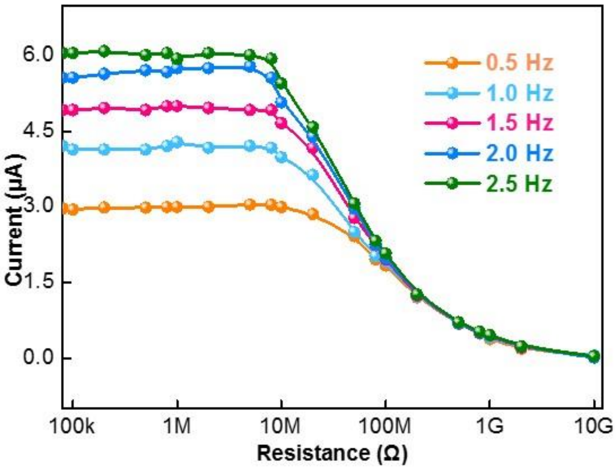

Figure S9. Influence of the load resistance on the magnitude of the output current at various working frequencies in taping mode.

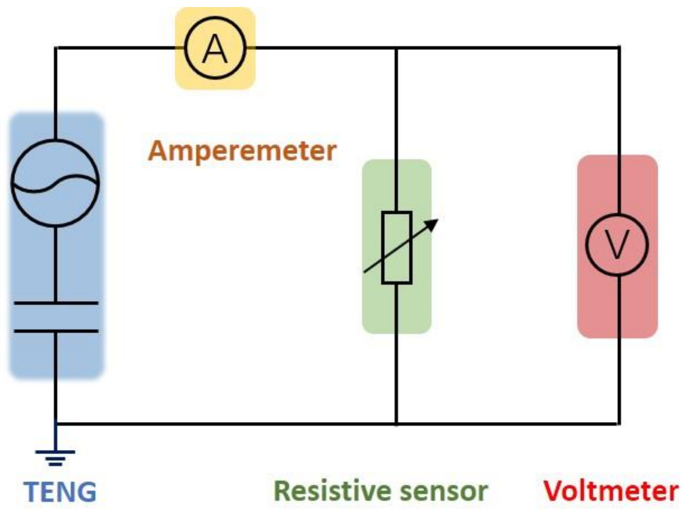

Figure S10. Equivalent circuit diagram for output measuring.

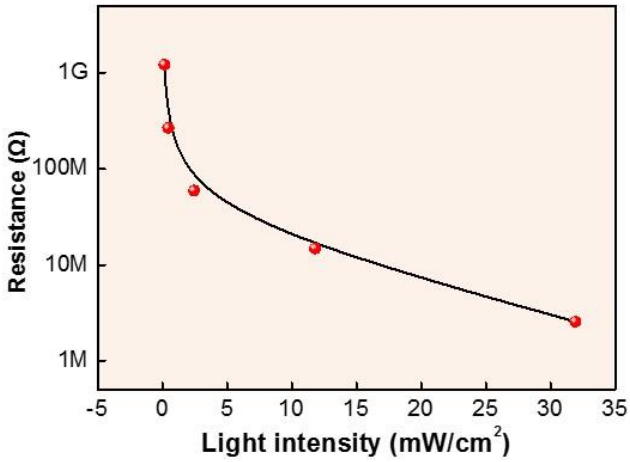

Figure S11. Resistance of the ZnO NPs UV photodetectors under 375 nm UV light with different power intensities irradiance.

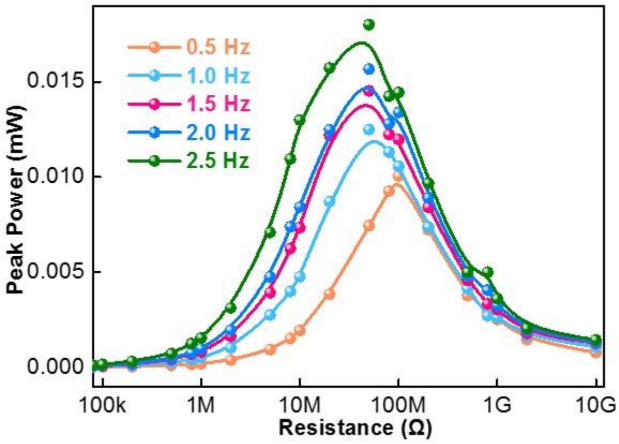

Figure S12. Peak power density under varies frequencies in sliding mode.

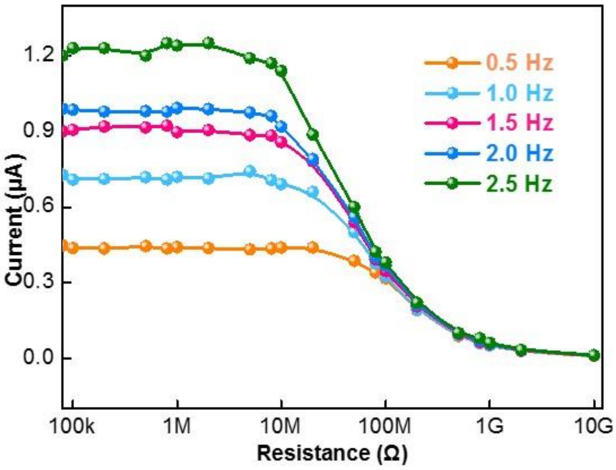

Figure S13. Influence of the load resistance on the magnitude of the output current at various working frequencies in sliding mode.

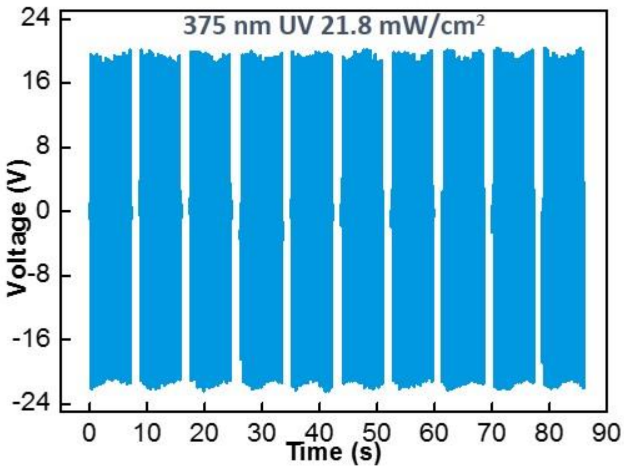

Figure S14. Stability test of self-powered UV detector under 375 nm UV light with power intensities irradiance of 21.8 mW/cm^2.

Supporting Note S1:

Firstly, when skin contacts with FEP film, electrons transfer from skin to FEP and generate equivalent positive and negative charges on the skin and FEP surface separately, as a consequence of the stronger electron affinities of FEP in state i. when the skin separates from the triboelectric surface, a potential difference generates between ITO electrode and the ground. In order to reach the electrostatic equilibrium, the electrons transfer from electrode to ground (state ii). Until the skin is far away from the surface, the charges on the skin have no electrostatic induction to the surface and the FEP and ITO electrode reach a new electrostatic equilibrium state (state iii). If the skin gets close to the surface again, there is an inverse electrons transfer between the electrode and ground (state iv).

Supporting Note S2:

In initial state, if the skin contact with the FEP film, the skin is easier to loss electrons to generate positive charges and FEP generates the equivalent negative charges. During the sliding process, the negative charges in the FEP films are at static state and the total electrostatic induced charges in the two electrodes are always 0. Firstly, the negative and positive charges are induced on the electrode one (E1) and electrode two (E2) as a result of the electrostatic induction (initial state). When the skin start to slide, the electrons flow from E1 to E2 via load circuit (intermediate state) and until sliding to the final state, the charge transfer process is finished. Then, the process goes to a new initial state and an inverse current generates in the load circuit.

Supporting Note S3:

When an external load resistance with impedance Z_{out} = R_{out} is applied, the voltage across the load resistance (V_{out}) shows as the following equation:

$$V_{out} = \frac{Z_{out}}{Z_{in}+Z_{out}} V_{OC} = \frac{R_{out}}{\frac{1}{2\pi f C_T}+R_{out}} V_{OC} \tag{S1}$$

where f is the frequency of the AC signal related to the mechanical motion, V_{OC} stands for the open-circuit voltage and C_T is the inherent capacitance.

In the circuit diagram (Figure 5a), the total load resistance is:

$$R_{out} = R_C + R_x \tag{S2}$$

where the Rc is the resistance of the constant resistor and Rx is the resistance of the UV photodetector.

The voltage across the constant resistor (R_C) is:

$$V_{Rc} = \frac{R_C}{R_C+R_x} V_{out} \tag{S3}$$

Combine the equation S1-S3, the divider voltage (V_{Rc}) across the constant resistors (R_C) shows as following equation:

$$V_{Rc} = \frac{R_C}{\frac{1}{2\pi f C_T}+R_C+R_x} V_{OC} \tag{S4}$$

According to this equation, it's easy to explain that the decrease of the resistance (R_x) leads to a higher V_{Rc}.